fig. 8). SM treatment resulted in a marked decrease in the normalized size ratio of the lateral wall. The decrease in the second turn was significant at $p < 0.001$ (Student's t test).

Discussion

The current study demonstrated that by decalcifying the bony wall of the cochlea with EDTA, the internal structures of the cochlea could be clearly visualized by OCT. The OCT images of the normal cochleae were significantly improved compared with those from previous reports [Wong et al., 2004; Lin et al., 2008; Sepehr et al., 2008; Subhash et al., 2010]. We found that OCT could prevent unnecessary misinterpretations due to artifacts introduced during the preparation of specimens for conventional histological examination. We could also demonstrate that three major cochlear pathologies, i.e. EH, hair cell degeneration and strial atrophy, could be clearly visualized by using OCT.

EH is commonly observed in patients with Ménière's disease and may also occur following head trauma or ear surgery, or in other inner ear disorders, allergies or systemic disorders such autoimmune disorders. The pathophysiology of Ménière's disease has been studied using animal models, and surgical ablation of the endolymphatic duct and sac of guinea pigs [Kimura and Schuknecht, 1965; Kimura, 1967] has most widely been used. It is impossible to determine the presence of EH by using physiological tests such as the auditory brainstem response or caloric test, since such examinations provide only information on the extent of damage to hearing or vestibular function. Thus, it is mandatory to evaluate the presence/absence and extent of EH by histological examination in animals. Schuknecht [1987, 1993] established a standard procedure for the morphological study of the human temporal bone that involved formalin fixation, EDTA decalcification, celloidin embedding and serial sectioning. Celloidin and paraffin are the two common embedding media used for histopathologic study of the human temporal bone by light microscopy. Although celloidin embedding permits excellent morphologic assessment, celloidin is difficult to remove, and there are significant restrictions on success with immunostaining. Other potential disadvantages of the use of celloidin include the length of time needed for embedment. Embedding in paraffin allows immunostaining to be performed, but the preservation of cellular detail within the membranous labyrinth is relatively poor [Merchant et al., 2006]. During the preparation process, the specimen must be embedded in a mold such as paraffin or celloidin, and such a process, especially with paraffin, is known to induce significant artifacts, making it difficult to evaluate the extent of EH. Compared with the OCT images in our study, paraffin-embedded HE specimens exhibited EH to a greater extent and also showed artifacts such as bending of the interscalar septum and basilar membrane and folding of Reissner's membrane. These findings suggest that estimating the extent of EH and associated tissue damage can be done more precisely using OCT images than by histological evaluation, especially using paraffin-embedded HE specimens. Further, the specimen can be easily used for molecular and immunohistochemical techniques after OCT imaging.

We also observed that OCT could visualize the degeneration of the organ of Corti, collapse of Reissner's membrane and strial atrophy 2 days after systemic administration of a combination of KM and EA and 4 weeks after perfusion with 20% SM throughout the cochlea. An intravenous administration of KM and EA induces hair cell degeneration and scar formation, which start 3 h after drug administration [Raphael and Altschuler, 1991]. In Raphael and Altschuler's report, mild flattening of the organ of Corti was seen from 9 h after drug administration. At this time, the outer hair cells from all three rows are replaced by supporting cells, which fill the entire space between the tunnel of Corti and Hensen cells. However, the inner hair cells are present and the shape of the organ of Corti is preserved. In our study, OCT could detect such degeneration as a reduction in the size of the organ of Corti, which could not be observed in the basal turn of an HE-stained section because of the artifacts produced (fig. 2a, b). Further, OCT could detect a mild collapse of Reissner's membrane, which again could not be detected in HE-stained sections. These findings suggest that estimating the extent of the degeneration of the organ of Corti and associated tissue damage (e.g. collapse of Reissner's membrane) can be done more precisely by using OCT images than histological evaluation, especially with paraffin-embedded HE specimens. Conversely, although OCT could detect severe degeneration of the organ of Corti, strial atrophy and remarkable collapse of Reissner's membrane in the SM group, it could not detect the loss of spiral ganglion cells, which could be observed in the HE specimens.

The method shown here cannot be applied to clinical evaluations of pathology in the cochlea. Therefore, we still need other novel technologies to improve the transparency and translucency of OCT.

Conclusions

By decalcifying the bony wall of the cochlea, we could clearly and widely visualize the internal structures of normal and pathological cochleae. We could easily manipulate the slice axis to obtain arbitrary plane views using OCT, and we could demonstrate EH, strial atrophy and damage to the organ of Corti as a distention of Reissner's membrane, a thinning of the lateral wall and a flattening of the organ of Corti, respectively. The OCT images of normal and pathological cochleae were virtually identical with those of HE specimens, except that the extent of EH was overestimated in histological images compared with OCT images and that there were several artifacts in the HE specimen, such as bending of the interscalar septum and basilar membrane, folding of Reissner's membrane, separation of the spiral ligament from the bony wall, and flattening of the organ of Corti in the basal turn, which were not seen in the OCT images. These findings indicate that observing the decalcified cochlea by using OCT would be of great value when examining cochlear pathology, especially EH, prior to or without histological examinations.

Disclosure Statement

This study was supported by a Health and Labor Science Research Grant for Research on Specific Diseases (Vestibular Disorders) from the Ministry of Health, Labor and Welfare of Japan, and by grants from the Ministry of Education, Science, Culture and Sports, Japan (No. 21592159) and by the Funding Program for Next Generation World-Leading Researchers (NEXT Program) of the Japan Society for the Promotion of Science (JSPS). We have no conflicts of financial interest in this paper.

References

Arnold W, Nadol JB Jr, Weidauer H: Ultrastructural histopathology in a case of human ototoxicity due to loop diuretics. Acta Otolaryngol 1981;91:399–414.

Brunschwig AS, Salt AN: Fixation-induced shrinkage of Reissner's membrane and its potential influence on the assessment of endolymph volume. Hear Res 1997;114:62–68.

Gates GA, Couropmitree NN, Myers RH: Genetic associations in age-related hearing thresholds. Arch Otolaryngol Head Neck Surg 1999; 125:654–659.

Hallpike CS, Cairns HWB: Observations of the pathology of Ménière's syndrome. Proc R Soc Med 1938;31:1317–1336.

Huang D, Swanson EA, Lin CP, Schuman JS, Stinson WG, Chang W, Hee MR, Flotte T, Gregory K, Puliafito CA, Fujimoto JG: Optical coherence tomography. Science 1991;254:1178–1181.

Izatt JA, Hee MR, Swanson EA, Lin CP, Huang D, Schuman JS, Puliafito CA, Fujimoto JG: Micrometer-scale resolution imaging of the anterior eye in vivo with optical coherence tomography. Arch Ophthalmol 1994;112:1584–1589.

Jang IK, Bouma BE, Kang DH, Park SJ, Park SW, Seung KB, Cho, KB, Shishkov M, Schlendorf K, Pomerantsev E, Houser SL, Aretz HT, Tearney GJ: Visualization of coronary atherosclerotic plaques in patients using optical coherence tomography: comparison with intravascular ultrasound. J Am Coll Cardiol 2002;39:604–609.

Kashio A, Sakamoto T, Suzukawa K, Asoh S, Ohta S, Yamasoba T: A protein derived from the fusion of TAT peptide and FNK, a Bcl-x_L derivative, prevents cochlear hair cell death from aminoglycoside ototoxicity in vivo. J Neurosci Res 2007;85:1403–1412.

Kimura RS: Experimental blockage of the endolymphatic duct and sac and its effect on the inner ear of the guinea pig. Ann Otol Rhinol Laryngol 1967;76:664–687.

Kimura RS, Schuknecht HF: Membranous hydrops in the inner ear of the guinea pig after obliteration of the endolymphatic sac. Pract Otorhinolaryngol (Basel) 1965;27:343–354.

Lin J, Staecker H, Jafri MS: Optical coherence tomography imaging of the inner ear: a feasibility study with implications for cochlear implantation. Ann Otol Rhinol Laryngol 2008; 117:341–346.

McGhan LJ, Merchant SN: Erythromycin ototoxicity. Otol Neurotol 2003;24:701–702.

Merchant SN, Burgess B, O'Malley J, Jones D, Adams JC: Polyester wax: a new embedding medium for the histopathologic study of human temporal bones. Laryngoscope 2006;116: 245–249.

Ohlemiller KK, Lett JM, Gagnon PM: Cellular correlates of age-related endocochlear potential reduction in a mouse model. Hear Res 2006;220:10–26.

Raphael Y, Altschuler RA: Scar formation after drug-induced cochlear insult. Hear Res 1991; 51:173–184.

Schuknecht H: Temporal bone collections in Europe and the United States: observations on a productive laboratory, pathologic findings of clinical relevance, and recommendations. Ann Otol Rhinol Laryngol 1987;130:1–19.

Schuknecht H: Methods of removal, preparation and study; in Schuknecht H (ed): Pathology of the Ear, ed 2. Philadelphia, Lea & Febiger, 1993, pp 1–29.

Schuknecht HF, Gacek MR: Cochlear pathology in presbycusis. Ann Otol Rhinol Laryngol 1993;102:1–16.

Sepehr A, Djalilian HR, Chang JE, Chen Z, Wong BJ: Optical coherence tomography of the cochlea in the porcine model. Laryngoscope 2008;118:1449–1451.

Shen B, Zuccaro G Jr: Optical coherence tomography in the gastrointestinal tract. Gastrointest Endosc Clin N Am 2004;14:555–571, x.

Slepecky N, Ulfendahl M: Glutaraldehyde induces cell shape changes in isolated outer hair cells from the inner ear. J Submicrosc Cytol Pathol 1988;20:37–45.

Subhash HM, Davila V, Sun H, Nguyen-Huynh AT, Nuttall AL, Wang RK: Volumetric in vivo imaging of intracochlear microstructures in mice by high-speed spectral domain optical coherence tomography. J Biomed Opt 2010; 15:036024.

Taylor RR, Nevill G, Forge A: Rapid hair cell loss: a mouse model for cochlear lesions. J Assoc Res Otolaryngol 2008;9:44–64.

Terayama Y, Kaneko Y, Kawamoto K, Sakai N: Ultrastructural changes of the nerve elements following disruption of the organ of Corti. I. Nerve elements in the organ of Corti. Acta Otolaryngol 1977;83:291–302.

Welzel J: Optical coherence tomography in dermatology. Skin Res Technol 2001;7:1–9.

Wong BJ, Jackson RP, Guo S, Ridgway JM, Mahmood U, Su J, Shibuya TY, Crumley RL, Gu M, Armstrong WB, Chen Z: In vivo optical coherence tomography of the human larynx: normative and benign pathology in 82 patients. Laryngoscope 2005;115:1904–1911.

Wong BJ, Zhao Y, Yamaguchi M, Nassif N, Chen Z, de Boer JF: Imaging the internal structure of the rat cochlea using optical coherence tomography at 0.827 μm and 1.3 μm. Otolaryngol Head Neck Surg 2004;130:334–338.

Xu SA, Shepherd RK, Chen Y, Clark GM: Profound hearing loss in the cat following the single co-administration of kanamycin and ethacrynic acid. Hear Res 1993;70:205–215.

Yamakawa K: Über die pathologische Veränderung bei einem Ménière-Kranken. J Otolaryngol Soc Jpn 1938;4:2310–2312.

Yamasoba T, Kondo K: Supporting cell proliferation after hair cell injury in mature guinea pig cochlea in vivo. Cell Tissue Res 2006;325:23–31.

Acta Oto-Laryngologica. 2013; 133: 1128–1132

informa
healthcare

ORIGINAL ARTICLE

Effects of EAS cochlear implantation surgery on vestibular function

KEITA TSUKADA[1], HIDEAKI MOTEKI[1,2], HISAKUNI FUKUOKA[1], SATOSHI IWASAKI[2] & SHIN-ICHI USAMI[1]

[1]*Department of Otolaryngology and* [2]*Department of Hearing Implant Science, Shinshu University School of Medicine, Matsumoto City, Japan*

Abstract

Conclusions: The patients who received electric acoustic stimulation (EAS) cochlear implantation had relatively good vestibular function compared with the patients who did not have residual hearing. The vestibular function was well preserved after atraumatic EAS surgery. The round window approach and soft electrode are preferred to decrease the risk of impairing vestibular function. *Objectives:* The aim of this study was to examine the characteristic features of vestibular functions before and after implantations in patients undergoing EAS. *Methods:* Vestibular functions in patients who underwent EAS implantation were examined by caloric testing and vestibular evoked myogenic potential (VEMP) in 11 patients before and in 13 patients after implantation. *Results:* Preoperative evaluation showed that of the 11 patients, most (73%) had good vestibular function. One of 11 patients (9%) had decreased response in postoperative VEMP but all of the patients had unchanged results in postoperative caloric testing.

Keywords: *Cochlear implant, VEMP, caloric test, preservation*

Introduction

Recently, a series of reports have shown the efficiency of electric acoustic stimulation (EAS) in patients with residual acoustic hearing in the lower frequencies [1]. The development of techniques such as soft surgery when performing cochleostomy [2], round window insertion [3], use of atraumatic electrodes [4,5], and postoperative steroid administration has enabled preservation of residual hearing after cochlear implantation (CI) surgery.

Current techniques of CI also facilitate remarkable improvement in hearing ability. However, consideration must still be given to the complications that can accompany a CI.

One possible such complication is impairment of vestibular function with resulting vertigo symptoms. The incidence of this complication as reported in the literature varies widely from 0.33% to 75% [6].

Although numerous studies have reported the effects of CI on the vestibular function in deaf patients, there have been no reports examining the vestibular function in patients who had residual hearing at lower frequencies, or of the postoperative effects on vestibular function of new atraumatic concepts of electrode and surgical techniques.

We recently published a preliminary report that the round window approach (RWA) is preferable from the viewpoint of vestibular function [7].

The aim of the present study was to further examine the changes in vestibular functions after implantation in patients who underwent EAS CI.

Material and methods

Patients

Thirteen patients (four males and nine females) who underwent EAS CI in our center were included in this

Correspondence: Shin-ichi Usami, Department of Otolaryngology, Shinshu University School of Medicine, 3-1-1, Asahi, Matsumoto City, 390-8621, Japan. Tel: +81 263 37 2666. Fax: +81 263 36 9164. E-mail: usami@shinshu-u.ac.jp

(Received 11 May 2013; accepted 30 June 2013)

ISSN 0001-6489 print/ISSN 1651-2251 online
DOI: 10.3109/00016489.2013.824110

study after obtaining informed written consent. The study was carried out with the approval of the Shinshu University Ethical Committee.

The age at implantation ranged from 30 to 60 years, and the mean age was 45.2 years. All patients fulfilled the following inclusion criteria: post-lingually acquired, bilateral sensorineural hearing loss (HL) with pure tone thresholds of <65 dB HL at the low frequencies (125, 250, and 500 Hz), of ≥80 dB HL at frequency 2 kHz, and of ≥85 dB HL at frequencies >4 kHz, and monosyllabic word recognition scores in quiet of ≤60% at 65 dB sound pressure level (SPL) in both ears in best-aided condition. Subjects were still included in this study if one of these frequencies was out of the mentioned decibel levels by only 10 dB or less.

Cochlear implantations

We performed CI with full insertion of the MED-EL FLEX$^{EAS®}$ electrode (MED-EL, Innsbruck, Austria) in all patients.

All surgeries were performed by a single surgeon and the RWA was applied for electrode insertion. Systemic antibiotics and dexamethasone were administered peri- and postoperatively. Residual hearing was successfully preserved in all patients (data not shown).

Vestibular testing

The patients were examined by caloric testing and vestibular evoked myogenic potential (VEMP) before or after implantation, or both, to obtain data on semicircular canal function and otolithic function, respectively.

In VEMP testing, electromyography (EMG) was carried out using a pair of surface electrodes mounted on the upper half and the sterna head of the sternocleidomastoid (SCM) muscle. The electrographic signal was recorded using a Neuropack evoked potential recorder (Nihon Kohden Co. Ltd, Tokyo, Japan). Clicks lasting for 0.1 ms at 105 dBnHL were presented through a headphone. The stimulation rate was 5 Hz, the bandpass filter intensity was 20–2000 Hz, and analysis time was 50 ms. The responses to 200 stimuli were averaged twice. Because the amplitude of the VEMP based on the unrectified EMG is correlated with the activity of the SCM muscle during the test [8], we measured the activity of the SCM muscle using the background integrated EMG response, the area under the averaged rectified EMG curve, from –20 ms to 0 ms before the sound stimulation. The correction of the amplitude was calculated as follows [9]:

Corrected amplitude (ms^{-1}) = amplitude of the averaged unrectified EMG (micro V)/background integrated EMG (micro V ms)

In caloric testing, maximum slow phase velocity (SPV) was measured by cold water irrigation (20°C, 5 ml, 20 s). We defined below 10°/s of SPV as areflexia and between 10 and 20°/s as hyporeflexia.

Statistical analysis

SPSS for Windows software (Chicago, IL, USA) was used for all analyses, and paired t test was applied when comparing differences in preoperative and postoperative vestibular functions. Statistical significance was set at $p < 0.05$.

Results

The results are summarized in Table I.

Semicircular canal function

Preoperative evaluation was performed bilaterally. Three of 11 patients (27%, nos 3, 4, and 5) showed areflexia or hyporeflexia in caloric testing. Patient no. 4 had bilateral areflexia, no. 5 had implanted ear areflexia and non-implanted ear hyporeflexia, and no. 3, had hypoflexia only in the non-implanted ear.

Postoperative caloric testing was obtained after 1 month or more. All 13 patients underwent postoperative caloric testing and 11 of them were also examined before the EAS implantations. Two (nos 4 and 5) of 13 patients (15%) had abnormal postoperative caloric test results in the implanted ear, although both of them also had abnormal results before implantations. Figure 1 shows the caloric response before and after EAS implantations for the implanted ear. Compared with before implantations, the results after implantations were unchanged in all of the 11 patients who underwent both preoperative and postoperative testing. One patient (no. 4) had areflexia both before and after implantation. The mean SPV was 28.06°/s preoperatively (SD = 17.61) and 28.68°/s postoperatively (SD = 15.53). There were no significant differences between results before and after implantations in caloric testing ($p = 0.67$).

Otolithic function

When preoperative evaluation was performed, no patients showed absent response in VEMP.

Postoperative VEMP was obtained after 1 month or more. All 13 patients underwent postoperative VEMP and 11 of them were also examined before EAS implantations. No patient had absent VEMP response

Table I. Summary of patients' details.

Patient no.	Age (years)/sex	Implanted side	Caloric test (°/s)				VEMP (ms^{-1})			
			Implanted ear		Non-implanted ear		Implanted ear		Non-implanted ear	
			Preop	Postop	Preop	Postop	Preop	Postop	Preop	Postop
1	41/M	R	NA	22.28	NA	20.74	NA	0.060	NA	0.068
2	47/F	L	NA	24.41	NA	9.09†	NA	0.029	NA	0.022
3	40/F	L	22.67	24.65	17.61*	17.76*	0.055	0.053	0.041	0.061
4	60/F	R	0†	0†	6.05†	0†	0.017	0.012	0.029	0.022
5	46/F	R	4.46†	8.31†	15.14*	19.94*	0.012	0.015	0.024	0.025
6	39/F	L	52.84	50	46.26	38.76	0.027	0.023	0.028	0.047
7	47/F	R	26.64	28.2	22.18	27.31	0.020	0.018	0.024	0.022
8	30/M	R	29.62	39.65	31.1	14.69	0.062	0.032	0.045	0.028
9	40/M	L	24.94	29.39	38.11	23.4	0.026	0.019	0.046	0.025
10	35/F	L	23.18	22.91	22.24	21.96	0.025	0.026	0.030	0.040
11	52/M	R	22.57	22.02	22.44	22.98	0.018	0.020	0.023	0.017
12	51/F	L	52.57	45.97	50.26	54.95	0.036	0.033	0.041	0.026
13	59/F	L	49.18	43.44	54.3	43.44	0.010	0.008	0.038	0.024

NA, not available.
*Hyporeflexia.
†Areflexia.

in the implanted ear. Figure 2 shows corrected VEMP amplitudes before and after EAS implantations for the implanted ear. Although one (no. 8) of the 11 patients (9%) had a decreased response in corrected VEMP amplitude, corrected VEMP amplitudes after implantations were unchanged in all but one of the patients, when compared with preoperative results. The mean corrected amplitude was 0.028 preoperatively (SD = 0.017) and 0.023 postoperatively (SD = 0.013). There were no significant differences between results before and after implantation in VEMP testing ($p = 0.095$).

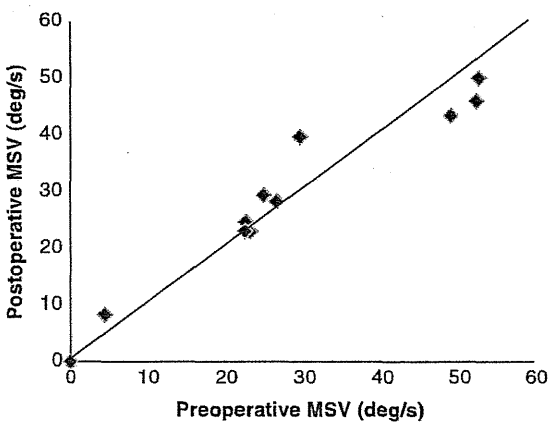

Figure 1. Results of caloric testing before and after EAS implantations in the implanted ear. There were no significant differences between preoperative and postoperative results ($p = 0.67$). MSV, maximum slow eye velocity.

Discussion

Previous reports showed that the frequencies of 'preoperative' vestibular disorders in profound hearing loss patients were about 30–73% in caloric testing [10–14] and about 11–65% in VEMP [10–15].

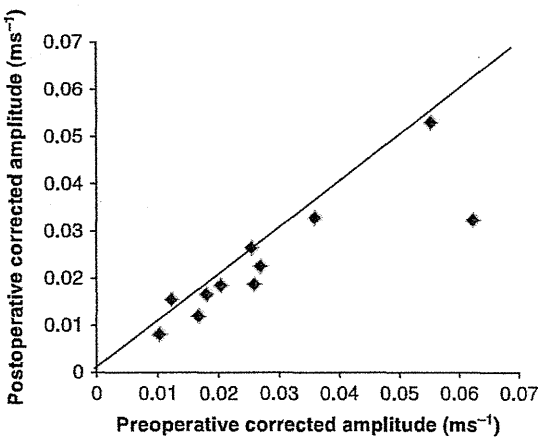

Figure 2. Results of VEMP before and after EAS implantations in the implanted ear. There were no significant differences between preoperative and postoperative results of VEMP testing in EAS implanted ears ($p = 0.095$). Corrected amplitude was used to compare the results.

In this study, we found that the 'preoperative' frequencies of vestibular disorders in hearing loss patients with residual hearing who received EAS were 27% and 0% in caloric testing and VEMP, respectively.

This finding suggested that vestibular function of the patients who underwent EAS was relatively good compared with the patients with profound hearing loss who underwent conventional CI.

In this study, to preserve such good vestibular function, atraumatic CI surgery (RWA with flexible thin electrode) was performed. Although one patient showed a decreased VEMP result, there was no hypofunction in postoperative caloric testing when compared with preoperative results in the implanted ear.

According to previous reports, various frequencies of postoperative deterioration in vestibular function were demonstrated. Postoperative hypofunction was found in 6–58% in the caloric testing [10–14,16–18], and 13–86% in VEMP [10–15]. One of the reasons for such variation is probably the surgical technique applied.

Todt et al. reported that hypofunction of postoperative VEMP was seen in 50% of patients who underwent cochleostomy and 13% of those with RWA Also, abnormal postoperative caloric testing results were seen in 42.9% of the patients who underwent cochleostomy and 9.4% of those who had the RWA [10].

Temporal bone studies have shown that an electrode insertion into the scala vestibuli involves damage of the osseous spiral lamina, basilar membrane, and vestibular receptors. The saccule was the most frequently damaged vestibular receptor, followed by the utricle and the semicircular canals [19].

However, when the electrode was inserted into the scala tympani, no vestibular damage was found [19]. Adunka et al. evaluated cochlear implant electrode insertions through the round window membrane histologically and reported that smooth implantations via round the window membrane resulted in deep, atraumatic insertions into the scala tympani [20]. Unintentional lesions to the basilar membrane can be avoided by using the round window as an exact anatomic landmark that is always in direct continuity with the scala tympani [20]. Previous histological and clinical studies clearly showed that the RWA is the technique that preserves the vestibular functions to the greatest extent and therefore is better than cochleostomy.

In the present study, the FLEX^{EAS} electrode was used for all of the patients. The cross-sectional diameter of the electrode is smaller than a conventional electrode, varying from 0.33 by 0.49 mm at the apex and to 0.8 mm at the basal, and a major feature of the device is its superior flexibility. Histology and dissection of human temporal bones performed by Adunka et al. confirmed the atraumatic character of this device [20]. Insertion forces with the conventional array and FLEX array were measured in an acrylic model of the scala tympani, demonstrating that insertion force could be reduced significantly by more than 40% with the FLEX^{EAS} electrode [4]. As in our previous study [7], such a smaller diameter and more flexible electrode might enable less damage to not only the cochlear tissue, but also the vestibular organs.

In conclusion, patients undergoing EAS implantation have good vestibular function compared with the vestibular function of the patients with profound hearing loss. It is important to preserve not only residual hearing but also the vestibular function of the implanted ears, using atraumatic surgical techniques. The RWA with soft electrode is preferable to decrease the risk of damage to vestibular function.

Acknowledgments

We thank A.C. Apple-Mathews for help in preparing the manuscript. This study was supported by a Health and Labour Sciences Research Grant for Comprehensive Research on Disability Health and Welfare from the Ministry of Health, Labour and Welfare of Japan (S.U.) and by a Grant-in-Aid for Scientific Research from the Ministry of Education, Science and Culture of Japan (S.U.).

Declaration of interest: The authors report no conflicts of interest. The authors alone are responsible for the content and writing of the paper.

References

[1] von Ilberg CA, Baumann U, Kiefer J, Tillein J, Adunka OF. Electric-acoustic stimulation of the auditory system: a review of the first decade. Audiol Neurootol 2011;16:1–30.

[2] Lehnhardt E, Laszig R. 1994. Specific surgical aspects of cochlear implant soft surgery. In Hochmair-Desoyer IJ, Hochmair ES, editors. Advances in cochlear implants. Vienna: Manz. p. 228–9.

[3] Skarzynski H, Lorens A, Piotrowska A, Anderson I. Preservation of low frequency hearing in partial deafness CI (PDCI) using the round window surgical approach. Acta Otolaryngol 2007;127:41–8.

[4] Adunka O, Kiefer J, Unkelbach MH, Lehnert T, Gstoettner W. Development and evaluation of an improved cochlear implant electrode design for electric acoustic stimulation. Laryngoscope 2004;114:1237–41.

[5] Baumgartner WD, Jappel A, Morera C, Gstöttner W, Müller J, Kiefer J, et al. Outcomes in adults implanted with the FLEXsoft electrode. Acta Otolaryngol 2007;127: 579–86.

[6] Buchman CA, Joy J, Hodges A, Telischi FF, Balkany TJ, Vestibular effects of CI. Laryngoscope 2004;114:1–22.
[7] Usami S, Moteki H, Suzuki N, Fukuoka H, Miyagawa M, Nishio SY, et al. Achievement of hearing preservation in the presence of an electrode covering the residual hearing region. Acta Otolaryngol 2011;131:405–12.
[8] Colebatch JG, Halmagyi GM, Skuse NF. Myogenic potentials generated by a click-evoked vestibulocollic reflex. J Neurol Neurosurg Psychiatry 1994;57:190–7.
[9] Shojaku H, Takemori S, Kobayashi K, Watanabe Y. Clinical usefulness of glycerol vestibular-evoked myogenic potentials: preliminary report. Acta Otolaryngol Suppl 2001;545:65–8.
[10] Todt I, Basta D, Ernst A. Does the surgical approach in cochlear implantation influence the occurrence of postoperative vertigo? Otolaryngol Head Neck Surg 2008;138:8–12.
[11] Melvin TA, Della Santina CC, Carey JP, Migliaccio AA. The effects of cochlear implantation on vestibular function. Otol Neurotol 2009;30:87–94.
[12] Krause E, Louza JP, Wechtenbruch J, Gürkov R. Influence of cochlear implantation on peripheral vestibular receptor function. Otolaryngol Head Neck Surg 2010;142:809–13.
[13] Krause E, Wechtenbruch J, Rader T, Gürkov R. Influence of cochlear implantation on sacculus function. Otolaryngol Head Neck Surg 2009;140:108–13.
[14] Wagner JH, Basta D, Wagner F, Seidl RO, Ernst A, Todt I. Vestibular and taste disorders after bilateral cochlear implantation. Eur Arch Otorhinolaryngol 2010;267:1849–54.
[15] Licameli G, Zhou G, Kenna MA. Disturbance of vestibular function attributable to cochlear implantation in children. Laryngoscope 2009;119:740–5.
[16] Krause E, Louza JP, Hempel JM, Wechtenbruch J, Rader T, Gürkov R. Effect of cochlear implantation on horizontal semicircular canal function. Eur Arch Otorhinolaryngol 2009;266:811–17.
[17] Fina M, Skinner M, Goebel JA, Piccirillo JF, Neely JG, Black O. Vestibular dysfunction after cochlear implantation. Otol Neurotol 2003;24:234–42.
[18] Enticott JC, Tari S, Koh SM, Dowell RC, O'Leary SJ. Cochlear implant and vestibular function. Otol Neurotol 2006;27:824–30.
[19] Tien HC, Linthicum FH Jr. Histopathologic changes in the vestibule after cochlear implantation. Otolaryngol Head Neck Surg 2002;127:260–4.
[20] Adunka O, Unkelbach MH, Mack M, Hambek M, Gstoettner W, Kiefer J. Cochlear implantation via the round window membrane minimizes damage to cochlear structures: a histologically controlled insertion study. Acta Otolaryngol 2004;124:807–12.

PLOS | ONE

Massively Parallel DNA Sequencing Successfully Identifies New Causative Mutations in Deafness Genes in Patients with Cochlear Implantation and EAS

Maiko Miyagawa[1], Shin-ya Nishio[1], Takuo Ikeda[2], Kunihiro Fukushima[3], Shin-ichi Usami[1]*

1 Department of Otorhinolaryngology, Shinshu University School of Medicine, Matsumoto, Japan, **2** Department of Otolaryngology, Tsudumigaura Handicapped Children's Hospital, Shunan, Japan, **3** Department of Otorhinolaryngology, Okayama University School of Medicine, Okayama, Japan

Abstract

Genetic factors, the most common etiology in severe to profound hearing loss, are one of the key determinants of Cochlear Implantation (CI) and Electric Acoustic Stimulation (EAS) outcomes. Satisfactory auditory performance after receiving a CI/EAS in patients with certain deafness gene mutations indicates that genetic testing would be helpful in predicting CI/EAS outcomes and deciding treatment choices. However, because of the extreme genetic heterogeneity of deafness, clinical application of genetic information still entails difficulties. Target exon sequencing using massively parallel DNA sequencing is a new powerful strategy to discover rare causative genes in Mendelian disorders such as deafness. We used massive sequencing of the exons of 58 target candidate genes to analyze 8 (4 early-onset, 4 late-onset) Japanese CI/EAS patients, who did not have mutations in commonly found genes including *GJB2*, *SLC26A4*, or mitochondrial 1555A>G or 3243A>G mutations. We successfully identified four rare causative mutations in the *MYO15A*, *TECTA*, *TMPRSS3*, and *ACTG1* genes in four patients who showed relatively good auditory performance with CI including EAS, suggesting that genetic testing may be able to predict the performance after implantation.

Citation: Miyagawa M, Nishio S-y, Ikeda T, Fukushima K, Usami S-i (2013) Massively Parallel DNA Sequencing Successfully Identifies New Causative Mutations in Deafness Genes in Patients with Cochlear Implantation and EAS. PLoS ONE 8(10): e75793. doi:10.1371/journal.pone.0075793

Editor: Akinori Kimura, Tokyo Medical and Dental University, Japan

Received July 16, 2013; **Accepted** August 21, 2013; **Published** October 9, 2013

Funding: This study was supported by a Health and Labour Sciences Research Grant for Comprehensive Research on Disability Health and Welfare from the Ministry of Health, Labour and Welfare of Japan (http://www.mhlw.go.jp/english/) (S.U.), and by a Grant-in-Aid for Scientific Research from the Ministry of Education, Science and Culture of Japan (http://www.mext.go.jp/english/) (S.U.). The funders had no role in study design, data collection and analysis, decision to publish, or preparation of the manuscript.

Competing Interests: All authors declare no competing interests.

* E-mail: usami@shinshu-u.ac.jp

Introduction

Cochlear Implantation (CI) has been established as a standardized therapy for severe to profound hearing loss [1]. Electric Acoustic Stimulation (EAS) is a hearing implant system combining a cochlear implant and acoustic amplification technology in one device, and has recently become a standard intervention for the patients with partial deafness, defined as a mild to moderate low-frequency sensorineural hearing loss sloping to a profound hearing loss in the higher frequencies [1]. One difficult point is that outcomes of CI/EAS are variable and many factors are thought to be involved in post-implantation performance. Satisfactory auditory performance in the patients with various deafness gene mutations indicates that genetic background would be helpful in predicting performance after CI [2]. When genetic background is involved in intra-cochlear etiology, there is potential for good performance. Therefore, it is important to identify the involved region inside/outside of the cochlea by identifying the responsible gene. Decisions as to whether to undergo EAS surgery and the timing of the surgery, as well as prediction of outcome after EAS is sometimes difficult because of individual differences in progression, which is sometimes of a rather rapid nature but sometimes rather stable. One advantage of genetic testing is that the possible prognosis for hearing, i.e., progressive or not, can be predicted for individual patients.

Etiological studies have shown genetic disorders to be a common cause of deafness, but difficulty lies in the fact that deafness is an extremely heterogenous disorder.

Invader-based multi-gene screening for 13 genes/46 mutations commonly found in Japanese, identified the responsible mutations in approximately 30% of deafness patients [3], accelerating the clinical application of gene screening. However, the etiology of the rest of the patients is still unknown. In addition, the involvement of at least 58 distinct genes sometimes makes the precise diagnosis difficult.

Targeted exon sequencing of selected genes using the Massively Parallel DNA Sequencing (MPS) technology will potentially enable us to systematically tackle previously intractable monogenic disorders and improve molecular diagnosis. We have recently reported that target exon sequencing using MPS is a powerful tool to identify rare gene mutations for deafness patients [4].

In this study, we have chosen 58 deafness-causative genes, and conducted genetic analysis using MPS-based genetic screening to find the rare genes responsible for the patients who received CI or EAS.

Subjects and Methods

Subjects

Eight deafness patients (4 early-onset, 4 late-onset) were randomly selected from among 150 CI or EAS patients (69 male and 81 female, aged 0 to 91), without common *GJB2, SLC26A4,* or mitochondrial 1555A>G or 3243A>G mutations determined by direct sequencing. Four patients with early-onset deafness received CI, and 4 late-onset patients had residual hearing at lower frequencies and received EAS. All subjects or next of kin, caretakers, or guardians on the behalf of the minors/children gave prior written informed consent for participation in the project, and the Ethical Committee of Shinshu University approved the study and the consent procedure.

Auditory behavioral development was assessed by IT-MAIS and LittlEARS, both of which are parent questionnaires regarding a young infant or toddler's auditory behavior [5,6]. IT-MAIS consists of 10 questions, each scored on a 5-point scale: 0 = never, 1 = rarely, 2 = occasionally, 3 = frequently, and 4 = always. LittlEARS has 35 questions, each scored as 1 = yes, and 0 = no.

Amplicon Library Preparation

An Amplicon library of the target exons was prepared with an Ion AmpliSeq™ Custom Panel (Applied Biosystems, Life Technologies., Carlsbad, CA) designed with Ion AmpliSeq™ Designer (https://www.ampliseq.com/browse.action) for 58 genes reported to be causative of non-syndromic hearing loss listed in Table S1 (Hereditary Hearing loss Homepage; http://hereditaryhearingloss.org/) by using Ion AmpliSeq™ Library Kit 2.0 (Applied Biosystems, Life Technologies) and Ion Xpress™ Barcode Adapter 1–16 Kit (Applied Biosystems, Life Technologies) according to the manufacturers' procedures.

In brief, DNA concentration was measured with Quant-iT™ dsDNA HS Assay (Invitrogen, Life Technologies) and Qubit® Fluorometer (Invitrogen, Life Technologies) and DNA quality was confirmed by agarose gel electrophoresis. 10 ng of each genomic DNA sample was amplified, using Ion AmpliSeq™ HiFi Master Mix (Applied Biosystems, Life Technologies) and AmpliSeq™ Custom primer pools, for 2 min at 99°C, followed by 15 two-step cycles of 99°C for 15 sec and 60°C for 4 min, ending with a holding period at 10°C in a PCR thermal cycler (Takara, Shiga, Japan). After the Multiplex PCR amplification, amplified DNA samples were digested with FuPa enzyme at 50°C for 10 min and 55°C for 10 min and the enzyme was successively inactivated for 60°C for 20 min incubation. After digestion, diluted barcode adapter mix including Ion Xpress™ Barcode Adapter and Ion P1 adaptor were ligated to the end of the digested amplicons with ligase in the kit for 30 min at 22°C and the ligase was successively inactivated at 60°C for 20 min incubation. Adaptor ligated amplicon libraries were purified with the Agencourt AMPure XP system (Beckman Coulter Genomics, Danvers, MA). The amplicon libraries were quantified by using Ion Library Quantitation Kit (Applied Biosystems, Life Technologies) and the StepOne plus realtime PCR system (Applied Biosystems, Life Technologies) according to the manufacturers' procedures. After quantification, each amplicon library was diluted to 20pM and the same amount of the 6 libraries for 6 patients were pooled for one sequence reaction.

Emulsion PCR and Sequencing

The emulsion PCR was carried out with the Ion OneTouch™ System and Ion OneTouch 200 Template Kit v2 (Life Technologies) according to the manufacturer's procedure (Publication Part Number 4478371 Rev. B Revision Date 13 June 2012). After the emulsion PCR, template-positive Ion Sphere™ Particles were enriched with the Dynabeads® MyOne™ Streptavidin C1 Beads (Life Technologies) and washed with Ion OneTouch™ Wash Solution in the kit. This process were performed using an Ion OneTouch™ ES system (Life Technologies).

After the Ion Sphere Particle preparation, MPS was performed with an Ion Torrent Personal Genome Machine (PGM) system using the Ion PGM™ 200 Sequencing Kit and Ion 318™ Chip (Life Technologies) according to the established procedures (Publication Part Number 4474596 Rev. B Revision Date 14 July 2012).

Base Call and Data Analysis

The sequence data were processed with standard Ion Torrent Suite™ Software and Torrent Server successively mapped to human genome sequence (build GRCh37/hg19) with Torrent Mapping Alignment Program optimized to Ion Torrent™ data. The average of 412.93 Mb sequences with about 3,200,000 reads was obtained by one Ion 318 chip. The 98.0% sequences were mapped to the human genome and 94.9% of them were on the target region. Average coverage of depth in the target region was 326.5 and 94.2% of them were over 20 coverage.

After the sequence mapping, the DNA variant regions were piled up with Torrent Variant Caller plug-in software. Selected variant candidates were filtered with the average base QV (minimum average base quality 25), variant frequency (40–60% for heterozygous mutations and 80–100% for homozygous mutations) and coverage of depth (minimum coverage of depth 10). After the filtrations, variant effects were analyzed with the wANNOVAR web site [7,8] (http://wannovar.usc.edu) including the functional prediction software for missense variants listed below. PhyloP (http://hgdownload.cse.ucsc.edu/goldenPath/hg18/phyloP44way/), Sorting Intolerant from Tolerant (SIFT; http://sift.jcvi.org/), Polymorphism Phenotyping (PolyPhen2; http://genetics.bwh.harvard.edu/pph2/), LRT (http://www.genetics.wustl.edu/jflab/lrt_query.html), MutationTaster (http://www.mutationtaster.org/), and GERP++ (http://mendel.stanford.edu/SidowLab/downloads/gerp/index.html).

Algorithm

Flow of informatics analysis is shown in Fig. 1. Missense, nonsense, and splicing variants were selected among the identified variants. Variants were further selected as less than 1% of, 1) the 1000 genome database (http://www.1000genomes.org/), 2) the 5400 exome variants (http://evs.gs.washington.edu/EVS/), and 3) the 72 in-house controls. Candidate mutations were confirmed by Sanger sequencing and the responsible mutations were identified by segregation analysis using samples from family members of the patients.

Direct Sequence Analysis

Primers were designed with the Primer 3 plus web server (http://www.bioinformatics.nl/cgi-bin/primer3plus/primer3plus.cgi). Each genomic DNA sample (40 ng) was amplified using AmpliTaq Gold (Life Technologies) for 5 min at 94°C, followed by 30 three-step cycles of 94°C for 30 sec, 60°C for 30 sec, and 72°C for 30 sec, with a final extension at 72°C for 5 min, ending with a holding period at 4°C in a PCR thermal cycler (Takara, Shiga, Japan). The PCR products were treated with ExoSAP I (GE Healthcare Bio, Buckinghamshire, UK) and by incubation at 37°C for 30 min, and inactivation at 80°C for 15 min. After the products were purified, we performed standard cycle sequencing reaction with ABI Big Dye terminators in an ABI 3130×l sequencer (Life Technologies).

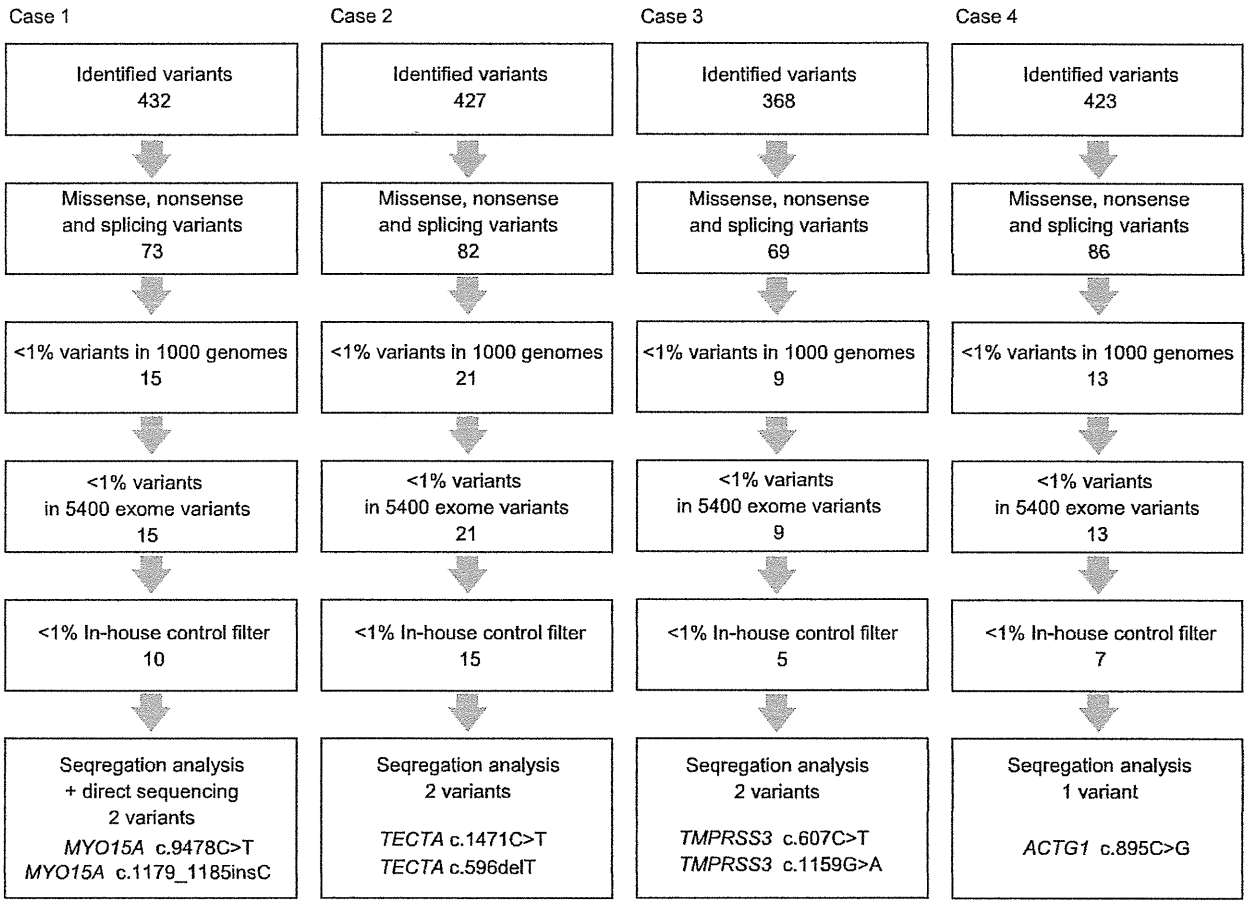

Figure 1. Flow of informatics analysis. Selected missense, nonsense, and splicing variants were filtered with 1) the 1000 genomes, 2) the 5400 exome variants, and 3) the in-house control. Responsible mutations were confirmed by segregation analysis.
doi:10.1371/journal.pone.0075793.g001

Results

After informatics analysis, several candidate variants were identified and segregation analysis confirmed responsible mutations in *MYO15A* (Case #1) and *TECTA* (Case #2) in pre-lingual patients with conventional CI, and mutations in *TMPRSS3* (Case #3) and *ACTG1* (Case #4) were identified in patients with post-lingual deafness with EAS (Fig. 1). All detected mutations were predicted to be pathologic by several software programs (Table 1). In the remaining four cases, there were no conclusive causative mutations found in this study.

Case #1: Severe Hearing Loss caused by *MYO15A* Mutations (Fig. 2)

As in Fig. 1, MPS identified 10 candidate variants in 9 genes. Among the 9 genes, *CDH23* and *MYO15A* are known to be inherited in a recessive manner. Sanger sequencing could not detect the *CDH23* variant. A *MYO15A* mutation (c.9478C>T (p.L3160F)) was confirmed by Sanger sequencing. Consecutive Sanger sequencing analysis identified another mutation, c.1179_1185insC, which was not found by MPS. The inconsistent results between the two methods were due to this mutation being located in the homo-polymer (poly C stretch) region, which is difficult to detect using this system [9] The patient (5y 5 m-old boy) had compound heterozygous *MYO15A* mutations (c.[9478C>T];[1179_1185insC]), and the parents were found to be carriers for these mutations (Fig. 2A). The frameshift mutation c.1179_1185insC, leading to a stop codon, was predicted to be causative, and the missense mutation, c.9478C>T, was predicted to be pathologic by several software programs (Table 1).

His hearing loss was found through newborn hearing screening using OAE. Auditory steady state response (ASSR) and conditioned orientation reflex (COR) evaluated at the ages of 1y 6 m, 2y 3 m, 2y 8 m, and 3y 6 m showed progressive hearing loss. He used hearing aids and some language development was seen, but due to progressive hearing loss, hearing aid amplification was insufficient, and he received a left CI (MEDEL PULSAR CI100/standard electrode) at the age of 4y 9 m. To obtain the final outcome, long-term follow up will be needed, but language was developed after 3 months of CI use (Scores of IT-MAIS: 16/40>25/40, LittlEar: 28>33).

Case #2: Profound Hearing Loss caused by *TECTA* Mutations (Fig. 3)

The patient (a 2-year-old boy) had compound heterozygous *TECTA* mutations (c.[596delT];[1471C>T]), and the parents were found to be carriers for these mutations (Fig. 3A). The frameshift mutation, c.596delT, leading to a stop codon, was predicted to be pathologic. The missense mutation, c.1471C>T

Table 1. Missense mutations found in this study.

Gene	Base Change	AA Change	ESP5400	1000g2012feb	dbSNP135	PhyloP	SIFT	PolyPhen2	LRT	MutationTaster	GERP++
MYO15A	c.9478C>T	p.L3160F	0.007618	0.01	rs140029076	N (0.885983)	D (0.97)	NA (0.754167)	NA (0.981216)	D (0.99518)	0.651
TECTA	c.1471C>T	p.R491C	–	–	–	C (0.998333)	D (0.97)	D (1)	D (1)	D (0.684828)	4.88
TMPRSS3	c.1159G>A	p.A387T	–	–	–	C (0.997807)	D (0.96)	B (0.074)	D (1)	N (0.364687)	4.62
ACTG1	c.895C>G	p.L299V	–	–	–	C (0.978424)	NA (0.750464)	B (0.006)	D (0.99998)	D (0.999635)	1.2

SIFT, Polyphen-2, PhyloP, LRT, Mutation Taster, and GERP++ are functional prediction scores in which increasing values indicate a probable mutation. ESP5400 and 100g2012feb are the allele frequency in each 5400 exome and 1000 genome project.
Abbreviations: C, conserved; N, not-conserved or neutral D, damaging or deleterious; B, benign; NA, not applicable.
doi:10.1371/journal.pone.0075793.t001

(p.R491C), was predicted to be pathologic by several software programs (Table 1).

His hearing loss was found through newborn hearing screening using OAE. ASSR and COR evaluated at the age of 8 m, 1 y 3 m, and 1 y 9 m showed progressive hearing loss. He used hearing aids, but due to insufficient amplification, he received a left CI at the age of 2. Language was developed after 4 months of CI use (Scores of IT-MAIS: 9/40>23/40).

Case#3: Late Onset Hearing Loss with Residual Hearing in Low Frequencies caused by *TMPRSS3* Mutations (Fig. 4)

The patient (a 40-year-old woman) had compound heterozygous *TMPRSS3* mutations c.[607C>T];[1159G>A] (p.[Q203X];[A387T]) (Fig. 4A). The nonsense mutation p.Q203X was predicted to be causative, and the missense mutation (p.A387T) was predicted to be pathologic by several software programs (Table 1). The parents were found to be carriers for these mutations. She had hearing loss detected by mass screening in primary school. It appeared to slowly progress, and by age 25 she suffered inconvenience in hearing and communication. EAS (MEDEL PULSAR FLEXeas) was applied at the ages of 38 and 39. Residual hearing for acoustic amplification could be preserved, and hearing level with bilateral EAS was around 30dB (Fig. 4C–E). Japanese monosyllable test (65dB SPL in quiet) showed dramatic improvement with bilateral EAS from 18% to 90% one year after receiving the second EAS (Fig. 4F).

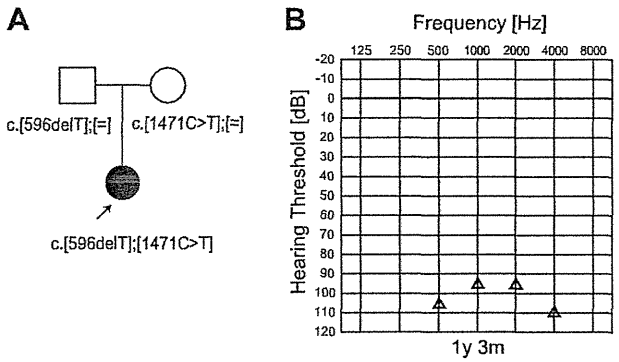

Figure 3. The CI patient with *TECTA* mutations. A: The patient has compound heterozygous *TECTA* mutations (c.[596delT];[1471C>T]), and the parents were found to be carriers for these mutations. B: COR audiogram finding (1y 9 m).
doi:10.1371/journal.pone.0075793.g003

Case #4: Late Onset Hearing Loss with Residual Hearing in Low Frequencies caused by *ACTG1* Mutation (Fig. 5)

The patient (a 41-year-old man) had a heterozygous *ACTG1* mutation, c.895C>G (p.L299V) (Fig. 5A). His pedigree was compatible with autosomal dominant hearing loss. A missense mutation, p.L299V, was predicted to be pathologic by several

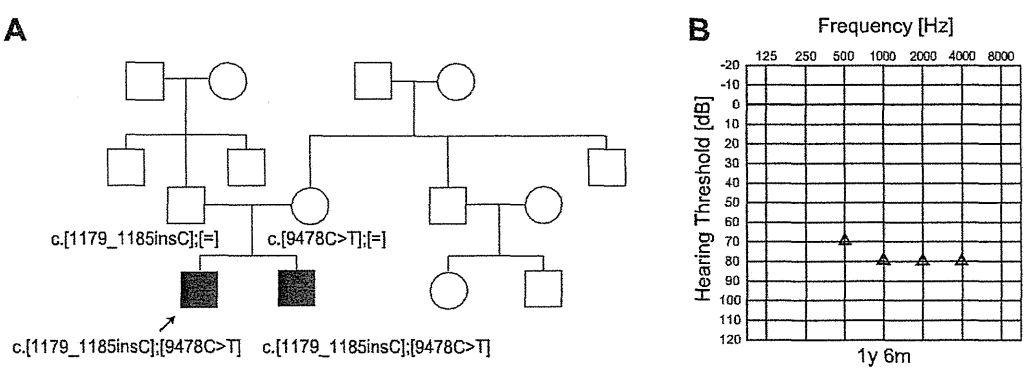

Figure 2. The CI patient with *MYO15A* mutations. A: The patient has compound heterozygous *MYO15A* mutations (c.[9478C>T];[1179_1185insC]), and the parents were found to be carriers for these mutations. B: COR audiogram finding (1y 6 m).
doi:10.1371/journal.pone.0075793.g002

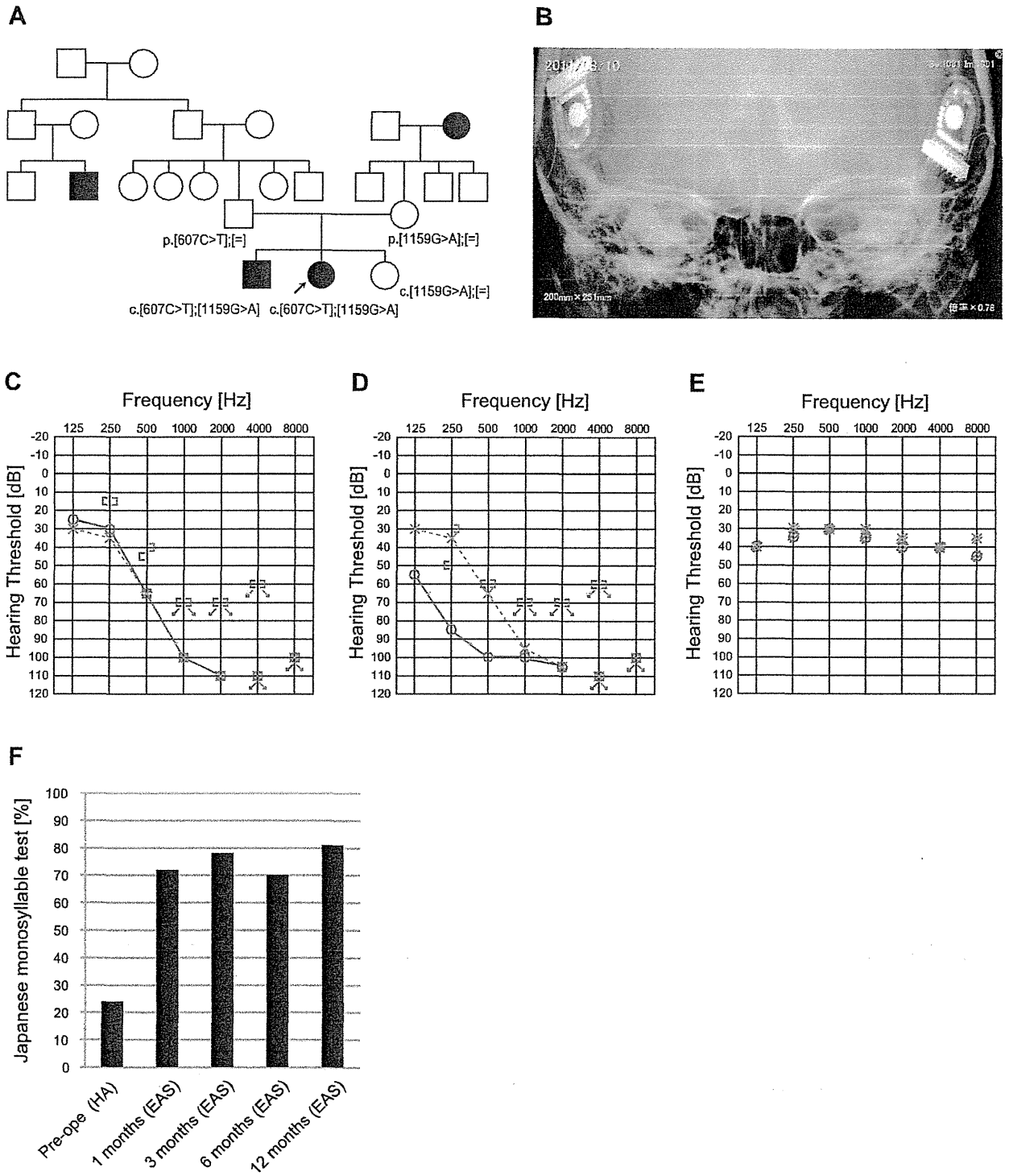

Figure 4. The EAS patient with *TMPRSS3* mutations. A: The patient has compound heterozygous *TMPRSS3* mutations, c.[607C>T];[1159G>A], and the parents were found to be carriers for these mutations. The patient's brother also has the same mutations. B: X-ray imaging after bilateral EAS. C: Pre-operative audiogram. D: Post-operative audiogram (left: 24 months after first EAS, right: 4 months after second EAS). E: Hearing threshold with bilateral EAS. F: Japanese monosyllable test (65dB SPL in quiet) showing dramatic improvement with bilateral EAS.
doi:10.1371/journal.pone.0075793.g004

software programs (Table 1). He noticed his hearing loss at around age 20. He received EAS due to progressive hearing loss. Residual hearing for acoustic amplification could be preserved, and hearing level with bilateral EAS was around 30dB (Fig. 5B, D, E). Japanese

monosyllable test (65dB SPL in quiet) showed dramatic improvement from 20% to 80% one year after receiving EAS (Fig. 5F). His father and brother carried the same mutation. The audiogram of the brother is shown in Fig. 5C. His father also has hearing loss based on anamnestic evaluation. Neither of the patient's sons (aged 10 and 12) have any hearing loss evaluated by pure tone audiogram, although the younger son has the same mutation.

Discussion

The present MPS-based genetic analysis efficiently identified rare causative mutations in four genes, *MYO15A*, *TECTA*, *TMPRSS3*, and *ACTG1*. All except *TMPRSS3* were first reported in patients with CI/EAS.

MYO15A has been reported mainly in severe to profound hearing loss [10]. Therefore, it is not surprising the patient with the *MYO15A* mutation was found among the CI patients. However, probably due to being too large to be screened by conventional direct sequencing, the routine screening of this particular gene was hampered in spite of its importance in this particular population. *MYO15A* is known to be responsible for DFNB3 [11]. *Myosin 15a* localizes to the tips of inner ear sensory cell stereocilia and is essential for staircase formation of the hair bundle [12]. Since the etiology is located within the sensory hair cells, comparatively better outcomes can be predicted. This case in fact showed better performance after CI.

TECTA encodes α-tectorin, the major component of non-collagenous glycoprotein of the tectorial membrane. *TECTA* has been reported to be responsible for both autosomal dominant non-syndromic sensorineural hearing loss (ADNSHL) (DFNA8/12) and autosomal recessive non-syndromic sensorineural hearing loss (ARNSHL) (DFNB21). Dominant *TECTA* mutations can cause mid-frequency, high-frequency progressive HL, and *TECTA* is reported to be the commonest causative gene among ADNSHL [13]. Dominant inherited deafness caused by this gene has not been reported to reach the level of profound hearing loss. In contrast, recessive *TECTA* mutations cause more profound hearing loss [14]. The etiology is located within the cochlea, therefore comparatively better outcomes can be predicted. This is the first report of a patient with mutations in this gene showing good outcome as prospected from intra-membranous labyrinth etiology.

In this study, *TMPRSS3* was identified in a patient with post-lingual deafness with EAS (Case #3).

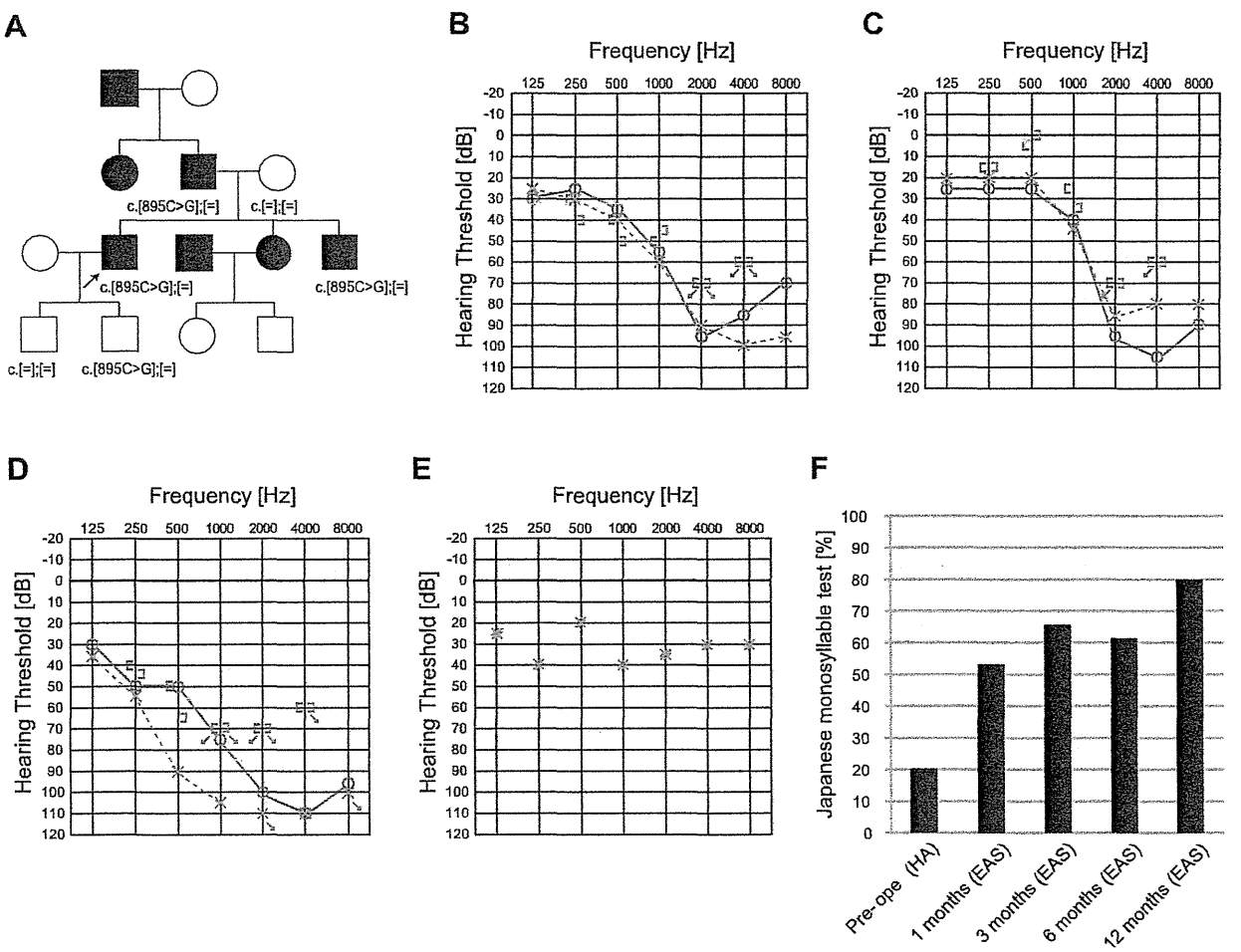

Figure 5. The EAS patient with *ACTG1* mutation. A: The patient has heterozygous *ACTG1* mutation, c.895C>G. Pedigree is compatible with autosomal dominant hearing loss. His father and brother carried the same mutation. B: Pre-operative audiogram. C: Audiogram of brother. D: Post-operative audiogram (6 months after EAS). E: Hearing threshold with EAS. F: Japanese monosyllable test (65dB SPL in quiet) showing dramatic improvement with EAS.

doi:10.1371/journal.pone.0075793.g005

TMPRSS3 is a member of the Type II Transmembrane Serine Protease family.

TMPRSS3 may be involved in processing proneurotrophins and therefore in the development and survival of the cochlear neurons [15].

TMPRSS3 has been reported to be responsible for DFNB8/10. Typically, the patients show ski-slope type audiograms and progressive HL [16], being compatible with the phenotype of the present patient. Outcome of CI for patients with *TMPRSS3* is controversial [2,16,17]. Two older papers reported good outcome of CI, while a recent report described poorer performance. Eppsteiner et al. [2] reported two cases of 58-year-old patients with a history of progressive hearing loss starting at the age of 5–6 years. Both of their outcomes were poorer compared with other patients, and the authors hypothesized that it was because the encoded protein is also expressed in the spiral ganglion. However, the present 40-year-old patient showed completely different performance after EAS, indicating that CI is not a contraindication and CI and/or EAS can be a recommended therapeutic option. Especially, the previously reported typical phenotype is high frequency involved hearing loss, which is a good indication for EAS. In the literature, there is also a severe phenotype with all frequencies affected [18]. Our 40-year-old patient did not have rapid progressive hearing loss (only 24 dB (125+250+500 Hz/3) during the 7-year follow-up period), supporting that this patient was a good candidate for EAS. Within this family, intra-familial variation was observed, i.e., an elder brother with the same mutations showed early onset (10 y.o.) profound hearing loss. Therefore, other factors may also potentially be involved in determining the phenotype (including severity and progression).

ACTG1 was identified in a patient with post-lingual deafness with EAS (Case #4).

His brother (35 y.o.) also showed similar high frequency involved progressive hearing loss. Together with the previous literature, high frequency involved progressive nature is one of the characteristic features of the patients with *ACTG1* mutations. The present study proved that EAS is a good therapeutic option for the patients with this gene mutation. *ACTG1* is known to be responsible for DFNA20/26. *ACTG1*, encoding gamma-actin, is the predominant actin isoform in auditory hair cells, more specifically in the cuticular plate, adherens junctions and stereocilia [19]. The etiology is located within the cochlea, therefore comparatively better outcomes can be predicted. Our patient's successful performance after EAS is compatible with the intra-membranous labyrinth etiology. The younger son who carried the same mutation will potentially have progressive hearing loss and his hearing is currently checked semiannually.

EAS is a new trend in therapy for the patients with residual hearing in the lower frequencies [20]. Various genes may be involved in the candidates [21], and we have found the mitochondrial 1555 A>G mutation and *CDH23* mutations in the patients receiving EAS [22], suggesting that the patients with those etiologies may have a potential to show good outcomes. Using the new MPS platform based on new generation sequencing enabled us to add two responsible genes, *TMPRSS3*, and *ACTG1*, in the patients with EAS. Identification of those genes may be good predictor when choosing the therapeutic options. Since the speed of progression may depend on the responsible gene, this information may be helpful for timing of EAS surgery and the selection of the electrode.

Overall, the current findings confirmed the importance of genetic information for predicting outcome of the CI/EAS patients, i.e., relatively good performance would be expected if the pathology exists within the cochlea. Such molecular diagnosis is important for the decision making process for selection of appropriate intervention, such as conventional cochlear implantation, EAS, hearing aid, or combination with other communication modes.

In spite of difficulty in discovery of the responsible gene for each individual patient, genetic testing using MPS may be a breakthrough. In the current series, MPS successfully discovered rare causative genes in CI patients and in EAS patients. These genes have not usually been screened and therefore mutations in them have not been diagnosed by the conventional approach. From that point of view, MPS has the potential power to identify such rare genes/mutations.

Supporting Information

Table S1 58 genes reported to be causative of non-syndromic hearing loss.
(PDF)

Acknowledgments

We thank A. C. Apple-Mathews for help in preparing the manuscript.

Author Contributions

Conceived and designed the experiments: SU. Performed the experiments: MM SN. Analyzed the data: MM SN. Contributed reagents/materials/analysis tools: MM TI KF. Wrote the paper: SU.

References

1. Wilson BS, Dorman MF (2008) Cochlear implants: a remarkable past and a brilliant future. Hear Res. 242: 3–21.
2. Eppsteiner RW, Shearer AE, Hildebrand MS, Deluca AP, Ji H, et al. (2012) Prediction of cochlear implant performance by genetic mutation: The spiral ganglion hypothesis. Hear Res. 292: 51–58.
3. Usami S, Nishio SY, Nagano M, Abe S, Yamaguchi T (2012) Deafness Gene Study Consortium: Simultaneous screening of multiple mutations by invader assay improves molecular diagnosis of hereditary hearing loss: a multicenter study. PLoS One. 7: e31276.
4. Miyagawa M, Naito T, Nishio SY, Kamatani N, Usami SI (2013) Targeted exon sequencing successfully discovers rare causative genes and clarifies the molecular epidemiology of Japanese deafness patients. PLoS ONE. *in press*.
5. Zimmerman-Phillips S, Osberger MJ, Robbins AM (1997) Infant-Toddler: Meaningful Auditory Integration Scale (IT-MAIS) Sylmar, CA: Advanced Bionics Corporation.
6. Coninx F, Weichbold V, Tsiakpini L (2003) LittlEARS Auditory Questionnaire. Innsbruck, Austria: MED-EL.
7. Chang X, Wang K (2012) wANNOVAR: annotating genetic variants for personal genomes via the web. J Med Genet. 49: 433–436.
8. Wang K, Li M, Hakonarson H (2010) ANNOVAR: functional annotation of genetic variants from high-throughput sequencing data. Nucleic Acids Research 38: e164.
9. Loman NJ, Misra RV, Dallman TJ, Constantinidou C, Gharbia SE, et al. (2012) Performance comparison of benchtop high-throughput sequencing platforms. Nat Biotechnol. 30: 434–439.
10. Liburd N, Ghosh M, Riazuddin S, Naz S, Khan S, et al. (2001) Novel mutations of *MYO15A* associated with profound deafness in consanguineous families and moderately severe hearing loss in a patient with Smith-Magenis syndrome. Hum Genet. 109: 535–541.
11. Wang A, Liang Y, Fridell RA, Probst FJ, Wilcox ER, et al. (1998) Association of unconventional myosin *MYO15* mutations with human nonsyndromic deafness DFNB3. Science 280: 1447–1451.
12. Belyantseva IA, Boger ET, Friedman TB (2003) Myosin XVa localizes to the tips of inner ear sensory cell stereocilia and is essential for staircase formation of the hair bundle. Proc Natl Acad Sci U S A. 100: 13958–13963.
13. Hildebrand MS, Morín M, Meyer NC, Mayo F, Modamio-Hoybjor S, et al. (2011) DFNA8/12 caused by *TECTA* mutations is the most identified subtype of nonsyndromic autosomal dominant hearing loss. Hum Mutat. 32: 825–834.
14. Mustapha M, Weil D, Chardenoux S, Elias S, El-Zir E, et al. (1999) An alpha-tectorin gene defect causes a newly identified autosomal recessive form of

sensorineural pre-lingual non-syndromic deafness, DFNB21. Hum Mol Genet. 8: 409–412.
15. Guipponi M, Vuagniaux G, Wattenhofer M, Shibuya K, Vazquez M, et al (2002) The transmembrane serine protease (*TMPRSS3*) mutated in deafness DFNB8/10 activates the epithelial sodium channel (ENaC) in vitro. Hum Mol Genet. 11: 2829–2836.
16. Weegerink NJ, Schraders M, Oostrik J, Huygen PL, Strom TM, et al. (2011) Genotype-phenotype correlation in DFNB8/10 families with TMPRSS3 mutations. J Assoc Res Otolaryngol. 12: 753–766.
17. Elbracht M, Senderek J, Eggermann T, Thürmer C, Park J, et al. (2007) Autosomal recessive post-lingual hearing loss (DFNB8): compound heterozygosity for two novel *TMPRSS3* mutations in German siblings. J Med Genet. 44: e81.
18. Wattenhofer M, Sahin-Calapoglu N, Andreasen D, Kalay E, Caylan R, et al. (2005) A novel TMPRSS3 missense mutation in a DFNB8/10 family prevents proteolytic activation of the protein. Hum Genet. 117: 528–535.
19. Morin M, Bryan KE, Mayo-Merino F, Goodyear R, Mencia A, et al. (2009) In vivo and in vitro effects of two novel gamma-actin (ACTG1) mutations that cause DFNA20/26 hearing impairment. Hum Mol Genet. 18: 3075–3089.
20. von Ilberg CA, Baumann U, Kiefer J, Tillein J, Adunka OF. (2011) Electric-acoustic stimulation of the auditory system: a review of the first decade. Audiol Neurootol. Suppl. 2: 1–30.
21. Usami S, Miyagawa M, Suzuki N, Moteki H, Nishio S, et al. (2010) Genetic background of candidates for EAS (Electric-Acoustic Stimulation). Audiol Med. 8: 28–32.
22. Usami S, Miyagawa M, Nishio SY, Moteki H, Takumi Y, et al. (2012) Patients with *CDH23* mutations and the 1555A>G mitochondrial mutation are good candidates for electric acoustic stimulation (EAS). Acta Otolaryngol. 132: 377–384.

OPEN ACCESS Freely available online

PLOS | ONE

Comprehensive Genetic Screening of *KCNQ4* in a Large Autosomal Dominant Nonsyndromic Hearing Loss Cohort: Genotype-Phenotype Correlations and a Founder Mutation

Takehiko Naito[1], Shin-ya Nishio[1], Yoh-ichiro Iwasa[1], Takuya Yano[1], Kozo Kumakawa[2], Satoko Abe[2], Kotaro Ishikawa[3], Hiromi Kojima[4], Atsushi Namba[5], Chie Oshikawa[6], Shin-ichi Usami[1]*

1 Department of Otorhinolaryngology, Shinshu University School of Medicine, Matsumoto, Japan, **2** Department of Otolaryngology, Toranomon Hospital, Tokyo, Japan, **3** Department of Otorhinolaryngology, Jichi Medical University, Tochigi, Japan, **4** Department of Otorhinolaryngology, Jikei University School of Medicine, Tokyo, Japan, **5** Department of Otorhinolaryngology, Hirosaki University School of Medicine, Hirosaki, Japan, **6** Department of Otorhinolaryngology, Kyushu University School of Medicine, Fukuoka, Japan

Abstract

The present study of *KCNQ4* mutations was carried out to 1) determine the prevalence by unbiased population-based genetic screening, 2) clarify the mutation spectrum and genotype/phenotype correlations, and 3) summarize clinical characteristics. In addition, a review of the reported mutations was performed for better understanding of this deafness gene. The screening using 287 probands from unbiased Japanese autosomal dominant nonsyndromic hearing loss (ADNSHL) families identified 19 families with 7 different disease causing mutations, indicating that the frequency is 6.62% (19/287). While the majority were private mutations, one particular recurrent mutation, c.211delC, was observed in 13 unrelated families. Haplotype analysis in the vicinity of c.211delC suggests existence of a common ancestor. The majority of the patients showed all frequency, but high-frequency predominant, sensorineural hearing loss. The present study adds a new typical audiogram configuration characterized by mid-frequency predominant hearing loss caused by the p.V230E mutation. A variant at the N-terminal site (c. 211delC) showed typical ski-slope type audiogram configuration. Concerning clinical features, onset age was from 3 to 40 years old, and mostly in the teens, and hearing loss was gradually progressive. Progressive nature is a common feature of patients with *KCNQ4* mutations regardless of the mutation type. In conclusion, *KCNQ4* mutations are frequent among ADNSHL patients, and therefore screening of the gene and molecular confirmation of these mutations have become important in the diagnosis of these conditions.

Citation: Naito T, Nishio S-y, Iwasa Y-i, Yano T, Kumakawa K, et al. (2013) Comprehensive Genetic Screening of *KCNQ4* in a Large Autosomal Dominant Nonsyndromic Hearing Loss Cohort: Genotype-Phenotype Correlations and a Founder Mutation. PLoS ONE 8(5): e63231. doi:10.1371/journal.pone.0063231

Editor: Klaus Brusgaard, Odense University hospital, Denmark

Received October 22, 2012; **Accepted** April 2, 2013; **Published** May 23, 2013

Funding: This study was supported by a Health and Labour Sciences Research Grant for Comprehensive Research on Disability Health and Welfare from the Ministry of Health, Labour and Welfare of Japan (http://www.mhlw.go.jp/english/) (S.U.), by the Acute Profound Deafness Research Committee of the Ministry of Health, Labour and Welfare of Japan (http://www.mhlw.go.jp/english/) (S.U.), by a Health and Labour Sciences Research Grant for Research on Specific Diseases (Vestibular Disorders) from the Japanese Ministry of Health, Labour and Welfare (http://www.mhlw.go.jp/english/) (S.U.), and by a Grant-in-Aid for Scientific Research from the Ministry of Education, Science and Culture of Japan (http://www.mext.go.jp/english/) (S.U.). The funders had no role in study design, data collection and analysis, decision to publish, or preparation of the manuscript.

Competing Interests: The authors have declared that no competing interests exist.

* E-mail: usami@shinshu-u.ac.jp

Introduction

Autosomal dominant nonsyndromic hearing loss (ADNSHL) is extremely heterogeneous. To date, more than 60 DFNA loci have been identified and 27 genes for DFNA have been identified (Van Camp G, Smith RJH. Hereditary Hearing Loss Homepage: http://hereditaryhearingloss.org). Genetic testing has become crucial for precise diagnosis, progression estimation, and selection of ideal intervention. However, due to such genetic heterogeneity and lack of recurrent mutations, routine genetic testing for ADNSHL has lagged. Linkage analysis is a powerful tool to identify a responsible gene for ADNSHL, but in the usual clinical setting, only a limited number of samples are available and this is insufficient for linkage analysis. Among ADNSHL genes, several are frequent, for example, *WFS1, KCNQ4, COCH, GJB2, MYO1A,* and *TECTA* [1]. Based on the number of reported mutations, the *KCNQ4* gene (responsible gene for DFNA2) is known to be one of the most frequent responsible genes for ADNSHL [1]. *KCNQ4*, a member of the voltage-gated potassium channel family, plays a role in potassium recycling in the inner ear [2]. In this 695-amino acid protein there are six transmembrane domains and a hydrophobic P-loop region, which is between the transmembrane domains S5 and S6 (residues 259 to 296). A channel pore, containing a potassium ion-selective filter, is formed by the P-loop domain. Channel function of this selectivity filter is eliminated by pore region mutations [2]. DFNA2-associated hearing loss has been reported to be typically late onset high frequency-involved and progressive over time, as opposed to early onset and severe loss in recessive forms [3]. To date, more than ten pathologic mutations have been identified in *KCNQ4* and they are mostly

missense mutations with a dominant-negative mechanism [3]. It was a matter of interest to know the prevalence of *KCNQ4* mutations to be found through unbiased population-based genetic screening. In this study, we performed the screening in a comprehensive manner to establish the mutation spectrum and genotype/phenotype correlations associated with this type of ADNSHL. Also, we were interested to know whether there are any recurrent mutations. In addition, we reviewed the reported mutations for better understanding of this deafness gene. We found that *KCNQ4* is frequent among ADNSHL patients, and therefore an important causative gene to be screened.

Materials and Methods

Subjects and clinical evaluation

The subjects participating in this study were 287 probands, each from an independent Japanese ADNSHL family. Whether or not progression was present was based on anamnestic evaluation. None of the subjects had any other associated neurological signs, visual dysfunction or diabetes mellitus. The control group was 252 unrelated Japanese individuals with normal hearing evaluated by auditory testing. The average threshold in the conversation frequencies (0.5 kHz, 1 kHz, 2 kHz) was calculated for the better ear, and severity of hearing loss was noted to be normal (−19 dB) in 24 subjects, mild (20–39 dB) in 69 subjects, moderate (40–69 dB) in 132 subjects, severe (70–94 dB) in 23 subjects, and profound (≥95 dB) in 24 subjects. Subjects with high frequency hearing loss only at 4 kHz and 8 kHz were classified as normal because they had normal hearing at 0.5, 1 and 2 kHz. Hearing loss severity was not obtained for 15 subjects. All probands' pure-tone thresholds were recorded on the frequencies of 125, 250, 500, 1000, 2000, 4000, and 8000 Hz.

Ethics Statement

All subjects or next of kin, caretakers, or guardians on the behalf of the minors/children gave prior written informed consent for participation in the project, and the Ethical Committee of Shinshu University approved the study and the consent procedure.

Mutation analysis

All fourteen exons and flanking intronic sequences of the *KCNQ4* gene were amplified by polymerase chain reaction PCR. Primers were designed to flank all of the exon-intron boundaries through use of the Primer3 web based server. Each genomic DNA sample (40 ng) was amplified using Multiplex PCR Assay Kit (Takara, Shiga, Japan) for 5 min at 95°C, followed by 40 three-step cycles of 94°C for 30 s, 60–67.6°C for 90 s, and 72°C for 90 s, with a final extension at 72°C for 10 min, ending with a holding period at 4°C in a Perkin-Elmer thermal cycler. The PCR products varied in size at about 100–400 bp, and they were treated with 0.1 ul exonuclease I (Amersham) and 1 ul shrimp alkaline phosphatase (Amersham) and by incubation at 37°C for 30 min, and inactivation at 80°C for 15 min. After the products were purified, we performed standard cycle sequencing reaction with ABI Big Dye terminators in an ABI 3100 autosequencer (Applied Biosystems).

Computer analysis to predict the effect of missense variants on the protein function was performed with wANNOVAR (http://wannovar.usc.edu) including the functional prediction software listed below. PhyloP (http://hgdownload.cse.ucsc.edu/goldenPath/hg18/phyloP44way/), Sorting Intolerant from Tolerant (SIFT; http://sift.jcvi.org/), Polymorphism Phenotyping (PolyPhen2; http://genetics.bwh.harvard.edu/pph2/), LRT (http://www.genetics.wustl.edu/jflab/lrt_query.html), and MutationTaster (http://www.mutationtaster.org/).

Haplotype analysis

Haplotype pattern within the 1Mbp region surrounding position c.211, where the frequent Japanese mutation c.211delC was found, was analyzed using a set of 48 single nucleotide polymorphisms (SNPs) (21 sites upstream and 27 sites downstream). Haplotype analysis was performed by the direct sequencing method described above.

Statistical analysis of progression of hearing loss

Each subject's ages at the time of examination and their pure tone thresholds were plotted for detailed progression analysis with 125, 250, 500, 1000, 2000, 4000, 8000 Hz, respectively. The average progressive rates of hearing loss (db/year) were calculated by linear regression lines, and analysis of difference of the rates was performed using analysis of covariance (ANCOVA) with SPSS ver19 software.

Results

Mutation analysis

Direct DNA sequencing identified 8 possible disease-causing mutations among 20 autosomal dominant families (Table 1). There were one deletion mutation (c.211delC), one insertion mutation (c.229_230*ins*GC), and 6 missense mutations (p.F182L, p.V230E, p.W276S, p.P291S, p.P291L, p.R297S) (Table 1). These included 5 novel and three previously reported pathologic mutations: c.211delC, p.F182L, and p.W276S (Table 1, Fig. 1). However, we excluded p.F182L as it is unlikely to be pathologic, according to the prediction program (Table 1). p.F182L was also found in a control sample with normal audiogram (Table 1). Therefore, 7 pathologic mutations from 19 families were found in a total of 287 ADNSHL families in this study (Fig. S1). Concerning the domains in which the 7 mutations were localized, 2 mutations were found in the N-terminal cytoplasmic domain, one mutation in the S4–S5 linker domain, 3 mutations in the pore region and the P-loop region, and one mutation in the S-6 transmembrane domain (Table 1, Fig. 1).

Frequency of KCNQ4 mutations

The frequency of *KCNQ4* mutations found in ADNSHL families in this study was 6.62% (19/287). The most prevalent mutation was c.211delC, at 4.53% (13/287) and it accounted for 68.4% (13/19) of all KCNQ4 mutations.

Haplotype analysis

Haplotype pattern within the 1Mbp region surrounding the position of the most frequent mutation c.211delC, was characterized using a set of 48 single nucleotide polymorphisms (SNPs) (21 sites upstream and 27 sites downstream). All patients from 6 families with c.211delC showed an exactly identical pattern in the allele with c.211delC, though the other allele showed a variety of haplotype patterns (Fig. 2).

Clinical characteristics

Table 2 summarizes clinical characteristics of 36 patients from 19 families with hearing loss caused by the *KCNQ4* mutations, including age at their first visit to the ENT clinic, onset age (age of awareness), audiogram configuration, progression of hearing loss, tinnitus, and vestibular symptoms. The ages at first clinic visits were from 0 to 78 years. Ages of onset (awareness age) ranged

Table 1. *KCNQ4* mutations found in this study together with previously reported mutations.

					Functional Prediction								
Nucleotide Change	**Amino Acid Change**	**Exon**	**Position**	**Alleles in Control Chr**	**SIFT**	**P2 D.S.**	**PhyloP**	**LRT**	**Mut Taster**	**GERP++**	**Study location**	**No of Fm**	**Reference**
c.211_223del13	p. Q71fs	1	N-term cyto	?	–	–	–	–	–	–	Belgium	1	Coucke, et al. (1999)
c.211delC	p. Q71fs	1	N-term cyto	0/252	–	–	–	–	–	–	Japan	14	Kamada, et al. (2006), This report
*** c.229_230insGC**	**p.H77fs**	**1**	**N-term cyto**	**0/252**	–	–	–	–	–	–	**Japan**	**1**	**This report**
c.546C>G	p.F182L	4	S3 trans	0/100, 1/252	T (0.00)	B (0.01)	C (0.97)	N (0.999853)	D (0.88)	3.43	Taiwan, Japan	3	Su, et al. (2007), This report
c.664_681del18	p.G215_220del6	4	S4-S5 linker	0/100	–	–	–	–	–	–	Korea	1	Baek, et al. (2010)
*** c.689T>A**	**p.V230E**	**4**	**S4–S5 linker**	**0/252**	**D (1.00)**	**D (0.97)**	**C (0.99)**	**D (0.999999)**	**D (0.99)**	**4.61**	**Japan**	**1**	**This report**
c.725G>A	p.W241X	5	S5 trans	0/100	–	–	–	–	–	–	USA	1	Hildebrand, et al. (2008)
c.778G>A	p.E260K	5	S5 trans	0/100	D (1.00)	D (0.99)	C (0.99)	D (1.00)	D (0.99)	4.73	USA	1	Hildebrand, et al. (2008)
c.785A>T	p.D262V	5	S5 trans	0/100	D (1.00)	D (0.99)	C (0.99)	D (1.00)	D (0.99)	4.73	USA	1	Hildebrand, et al. (2008)
c.821T>A	p.L274H	5	PR (P)	?	D (1.00)	D (0.99)	C (0.99)	D (1.00)	D (1.00)	4.73	Neth	2	Van Hauwe, et al. (2000), De Heer, et al. (2011)
c.827G>C	p.W276S	5	PR (P)	0/252	D (1.00)	D (1.00)	C (0.99)	D (1.00)	D (1.00)	4.73	Neth, Japan	4	Coucke, et al. (1999), Akita et al. (2001), Van Camp, et al. (2002), Topsakal, et al. (2005)
c.842T>C	p.L281S	6	PR (P)	0/96	D (1.00)	Pr (0.84)	C (0.99)	D (1.00)	D (1.00)	5.14	USA	1	Talebizadeh, et al. (1999)
c.853G>T	p.G285C	6	PR (P)	?	D (1.00)	D (1.00)	C (0.99)	D (0.999999)	D (1.00)	5.14	USA	1	Coucke, et al. (1999)
c.853G>A	p.G285S	6	PR (P)	0/150	D (1.00)	D (0.99)	C (0.99)	D (0.999999)	D (1.00)	5.14	France	1	Kubisch, et al. (1999)
c.859G>C	p.G287R	6	PR (P)	0/274	D (1.00)	D (0.99)	C (0.99)	D (1.00)	D (1.00)	5.14	USA	1	Arnett, et al. (2011)
*** c.871C>T**	**p.P291S**	**6**	**PR (P)**	**0/252**	**D (1.00)**	**D (1.00)**	**C (0.99)**	**D (1.00)**	**D (1.00)**	**5.14**	**Japan**	**1**	**This report**
*** c.872C>T**	**p.P291L**	**6**	**PR (P)**	**0/252**	**D (1.00)**	**D (1.00)**	**C (0.99)**	**D (1.00)**	**D (1.00)**	**5.14**	**Japan**	**1**	**This report**
c.886G>A	p.G296S	6	PR	0/100	D (0.99)	D (0.97)	C (0.99)	D (1.00)	D (0.99)	5.14	Spain	1	Mencia, et al. (2008)
*** c.891G>T**	**p.R297S**	**6**	**S6 trans**	**0/252**	**D (1.00)**	**D (0.99)**	**C (0.99)**	**D (1.00)**	**D (0.95)**	**3.89**	**Japan**	**1**	**This report**
c.961G>A	p.G321S	7	S6 trans	?	D (0.99)	Po (0.31)	C (0.99)	D (1.00)	D (0.99)	4.92	Neth	1	Coucke, et al. (1999)

SIFT, Polyphen-2, PhyloP, LRT, Mutation Taster, and GERP++ are functional prediction scores in which increasing values indicate a probable mutation.

Abbreviations: Chr, chromosomes; P2, PolyPhen2; MutTaser, Mutation Taser; Fm, family; cyto, cytoplasmic; trans, transmembrane; PR, Pore region; (P), P-loop; T, tolerated; D, damaging or deleterious; B, benign; Pr, probably damaging; Po, possibly damaging; C, conserved; N, neutral. Neth, Netherlands; *, Novel mutations found in this study.

doi:10.1371/journal.pone.0063231.t001

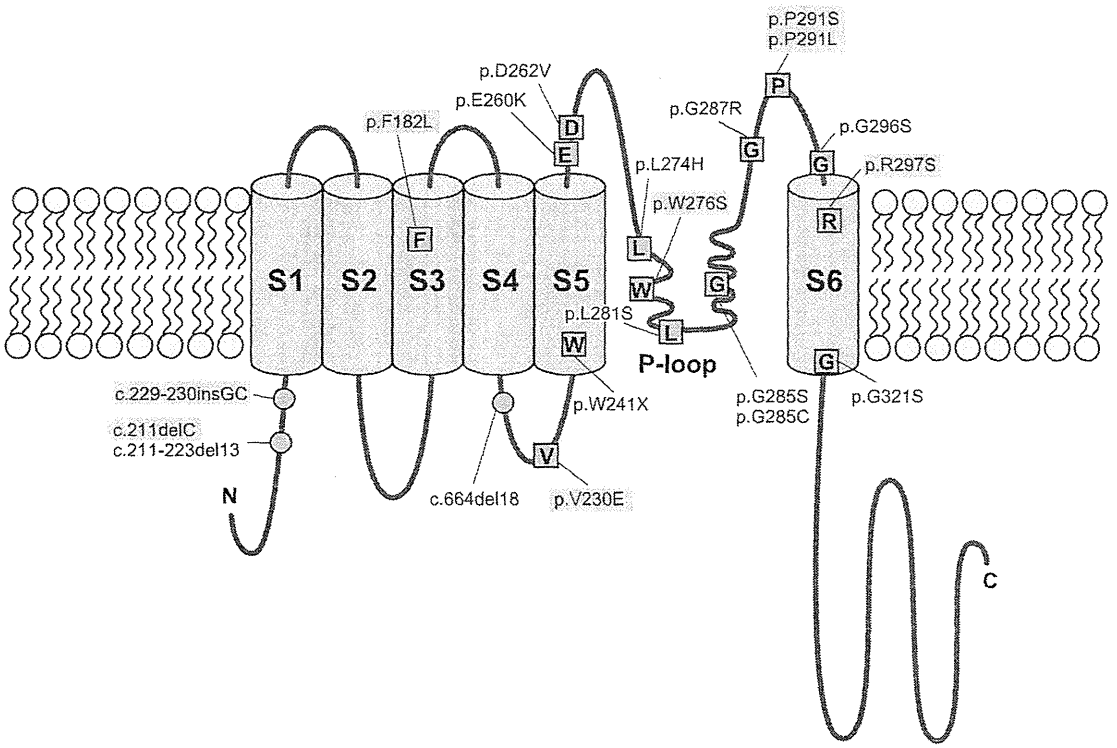

Figure 1. Localization of 20 *KCNQ4* mutations reported in previous studies in the protein. The 6 transmembrane domains (S1–S6) and the P-loop, located between S5 and S6, are shown. 5 mutations are concentrated in a narrow P-loop range. Mutations with pink and blue shadows; possible mutations detected in this study. Blue indicates novel mutations. Original schema is modified from Mencia A (2008) [14].
doi:10.1371/journal.pone.0063231.g001

from 3 to 40 years old, though the majority became aware when in their teens or younger. Most patients had associated tinnitus, but no vestibular symptoms except in a few cases.

Genotype/phenotype correlations

Concerning type of hearing loss, there were some correlations between genotype and phenotype (audiogram configuration). A variant at the N-terminal site (c. 211delC) showed ski-slope type configuration of audiogram with usually nearly normal hearing at 125–1000 Hz. We found this mutation in 20 patients from 13 families and their overlapped audiogram confirmed a similar configuration (Fig. 3). Onset age was from 10 to 40 years old, with most being in theirs teens and hearing loss was gradually progressive with age (Fig. 3, Table 2). The patients who had a variant in the P-loop region (W276S, P291L, P291S) also had high frequency involved hearing loss, but with some deterioration in the lower frequencies as well (Fig. 3). Most of the patients had earlier onset compared to the former phenotype and a progressive nature (Fig. 3, Table 2). The third audiogram configuration was mid-frequency involved hearing loss found in a family with a variant in the S4–S5 linker region (V230E) (Fig. 3). In most family members, onset was before age ten and gradually progressive (Fig. 3, Table 2). Overlapped audiograms were made for three mutations (W276S, c.211delC, V230E) for which there was a large enough number of patients to be analyzed (Fig. 3).

Therapeutic intervention

Sufficient amplification of hearing aids was obtained in all patients, and no patients received cochlear implantation. An affected subject with W276S (Family-Patient No. 16–2 in Table 2) had used a hearing aid from age 29. Similarly, affected subjects with P291L (Family-Patient No. 18–1) and V230E (Family-Patient No. 15–2) had used hearing aids. None of the affected subjects with c.211delC had a history of hearing aid usage.

Progression analysis

Detailed progression analysis in each frequency showed each affected member's age and their pure tone thresholds for 125, 250, 500, 1000, 2000, 4000, 8000 Hz, respectively (Fig. 4). Linear regression lines calculated by the plots are shown in the graph. Regarding the average progressive rates of hearing loss (db/year) for the patients with c.211delC, 125 (0.15) and 250 Hz (0.078) were shown to be significantly stable compared to the other two mutations (ANCOVA: $p<0.05$). They exhibited milder hearing loss at 500 and 1 KHz (ANCOVA: $p<0.05$). In contrast, at 4 KHz and 8 KHz, the patients with V230E mutations showed milder hearing loss compared to the other two mutations (ANCOVA: $p<0.05$).

Discussion

In this study, we have conducted a comprehensive genetic screening of *KCNQ4* using a large cohort of Japanese ADNSHL patients to establish the mutation spectrum. The *KCNQ4* mutations found in this study together with previously reported mutations (summarized in Table 1) represent an up-dated mutation spectrum for this gene. For missense mutations, we have gone through all reported missense mutations by computer analysis programs, SIFT and PolyPhen2, to predict the effect of

Distance from the c.211delC mutation (bp)	Fm 1		Fm2	Fm 5		Fm 10		Fm 11		Fm 13				Allele frequency				Marker
	Fa (+)	Dau (+)	Dau (+)	Mo (+)	Son (+)	Mo (+)	Son (+)	g.M (+)	Mo (+)	g.M (+)	Mo (+)	Son (+)	Dau (+)					
490912	C	C	T	T	T	C/T	C/T	C	C	T	T	T	T	C	0.80	T	0.20	rs10489431
468938	T	T	T	C/T	C/T	C/T	C/T	T	T	T	T	T	T	C	0.47	T	0.53	rs1846158
441312	A	A	A	A	A	A	A	A	A	A	A	A	A	T	0.31	A	0.69	rs12088482
422378	G	G	G	G	G	G	G	G	G	G	G	G	G	A	0.27	G	0.73	rs3013462
372705	A	A	A/G	A	A	A	A	A	A	A	A	A	A	G	0.68	A	0.32	rs16827291
339980	C	C	C	C/G	C/G	C/G	C/G	C	C	C	C	C	C	G	0.76	C	0.24	rs10489433
333758	C/T	C/T	C/T	C/T	C/T	C/T	C/T	C	C	C	C	C	C	T	0.44	C	0.56	rs209607
333573	G	G	G	G	G	G	G	G	G	G	G	G	G	G	0.89	A	0.11	rs2076493
285371	C/G	C/G	C	C	C	C	C	C	C	C	C	C	C	C	0.48	G	0.52	rs12034162
215165	C/T	C/T	T	T	T	T	T	T	T	T	T	T	T	T	0.44	C	0.56	rs4660167
207908	G	G	G	G	G	A/G	A/G	A/G	A/G	G	G	G	G	G	0.41	A	0.59	rs4660436
201218	C/T	C/T	T	T	T	C/T	C/T	C/T	C/T	T	T	T	T	T	0.36	C	0.64	rs12128397
174767	G	G	G	G	G	G	G	G	G	G	G	G	G	G	0.59	A	0.41	rs500586
173410	A	A	A	A/G	A/G	A	A	A	A	A	A	A	A	G	0.56	A	0.44	rs12217146
168622	G	G	G	G	G	G	G	G	G	G	G	G	G	G	0.60	C	0.40	rs504242
151498	T	T	T	C/T	C/T	T	T	T	T	T	T	T	T	T	0.61	C	0.39	rs542214
140107	C	C	C	C/T	C/T	C	C	C	C	C	C	C	C	C	0.62	T	0.38	rs7520394
9505	T	T	T	T	T	T	T	T	T	T	T	T	T	A	0.42	T	0.58	rs823674
6548	C	C	C	C	C	C	C	C	C	C	C	C	C	T	0.39	C	0.61	rs1327887
3196	A	A	A	A/G	A/G	A	A	A	A	A	A	A	A	G	0.63	A	0.37	rs12405252
2353	T	T	T	T	T	T	T	T	T	T	T	T	T	T	0.70	C	0.30	rs17361386
0	--	--	--	--	--	--	--	--	--	--	--	--	--	-	--	-	--	c.211delC
17282	C	C	C	C	C	C	C	C	C	C/T	C/T	C/T	C/T	C	0.23	T	0.77	rs4660464
20187	A	A	A/T	A/T	A/T	A/T	A/T	A	A	A	A	A	A	T	0.87	A	0.13	rs12408769
25343	G	G	G	C/G	C/G	G	G	G	G	G	G	G	G	G	0.70	C	0.30	rs878043
34533	G	G	G	G	G	G	G	G	G	G	G	G	G	G	0.58	C	0.42	rs2361658
41555	A	A	A/G	A/G	A/G	A	A	A	A	A	A	A	A	A	0.50	G	0.50	rs3767942
43025	A	A	A	A/G	A/G	A/G	A/G	A	A	A	A	A	A	G	0.76	A	0.24	rs6697721
43513	T	T	C/T	C/T	C/T	T	T	T	T	T	T	T	T	T	0.73	C	0.27	rs3767944
43673	T	T	C/T	C/T	C/T	C/T	C/T	T	T	T	T	T	T	C	0.79	T	0.21	rs4660176
58166	C/T	C/T	T	C/T	C/T	T	T	T	T	T	T	T	T	C	0.23	T	0.77	rs1576122
58742	A	A	A/G	A	A	A	A	A	A	A	A	A	A	A	0.64	G	0.36	rs4660472
61431	A/C	A/C	A	A/C	A/C	A/C	A/C	A	A	A	A	A	A	C	0.33	A	0.67	rs4534368
65688	T	T	T	C/T	C/T	T	T	T	T	T	T	T	T	C	0.37	T	0.63	rs11209014
68464	A	A	G	A/G	A/G	A/G	A/G	G	G	G	G	G	G	A	0.46	G	0.55	rs4660473
73906	T	T	T	T	T	T	T	T	T	T	T	T	T	C	0.21	T	0.80	rs913382
75825	G	G	A	A/G	A/G	A	A	A	A	A	A	A	A	G	0.47	A	0.53	rs11209041
101565	A	A	A/T	T	T	A/T	A/T	T	T	A/T	A/T	A/T	A/T	T	0.60	A	0.40	rs6700929
121363	T	T	T	T	T	T	T	T	T	T	T	T	T	T	0.52	C	0.48	rs6684543
122261	T	T	T	T	T	T	T	C	C	T	T	T	T	C	0.68	T	0.32	rs11209145
233975	G	G	C	C/G	C/G	C/G	C/G	G	G	C	C	C	C	G	0.77	C	0.23	rs11209361
237645	A	A	C	A/C	A/C	A/C	A/C	A	A	C	C	C	C	A	0.86	C	0.14	rs6674450
250602	A	A	T	A/T	A/T	A/T	A/T	A	A	T	T	T	T	A	0.84	T	0.16	rs11580656
274693	A	A	A	A	A	A	A	A	A	A	A	A	A	G	0.09	A	0.91	rs4660500
322363	T	T	G/T	G/T	G/T	G/T	G/T	T	T	G	G	G	G	G	0.43	T	0.57	rs548007
334776	G	G	A	A/G	A/G	A	A	G	G	A	A	A	A	G	0.84	A	0.16	rs2284802
369918	G	G	A	A/G	A/G	A/G	A/G	G	G	A	A	A	A	A	0.23	G	0.77	rs213744
487513	C	C	C/T	C/T	C/T	T	T	C	C	T	T	T	T	C	0.48	T	0.52	rs11209779
503189	G	G	G	G	G	G	G	G	G	G	G	G	G	G	0.73	A	0.27	rs12029950

*Fm (n), Family number (n); Mo, Mother; Fa, Father; Dau, Daughter, g. M, grand mother,